

Original Article

Hydroxysafflor yellow A promotes multiterritory perforating flap survival: an experimental study

Chenxi Zhang^{1,2,3*}, Zhenxuan Shao^{1,2,3*}, Zhentai Chen^{1,2,3}, Chen Lin^{1,2,3}, Sunli Hu^{1,2,3}, Zhiling Lou^{1,2,3}, Jiafeng Li^{1,2,3}, Xuanqi Zheng^{1,2,3}, Nan Lin^{1,2,3}, Weiyang Gao^{1,2}

¹Department of Orthopaedics, The Second Affiliated Hospital and Yuying Children's Hospital of Wenzhou Medical University, Wenzhou 325000, Zhejiang, P. R. China; ²Zhejiang Provincial Key Laboratory of Orthopaedics, Wenzhou 325000, Zhejiang, P. R. China; ³The Second Clinical Medical College of Wenzhou Medical University, Wenzhou 325027, P. R. China. *Equal contributors.

Received March 17, 2020; Accepted July 16, 2020; Epub August 15, 2020; Published August 30, 2020

Abstract: The use of perforator flaps is a common surgical technique in wound repair. However, the area surrounding the multiterritory perforating flap often becomes necrotic due to ischemia. Hydroxysafflor yellow A (HSYA), a traditional Chinese medicine extracted from edible safflower, can be used medicinally to promote angiogenesis, inhibit apoptosis, and alleviate oxidative stress and other biological activities. Here, we investigated the effect of HSYA on perforator flap survival and its potential mechanism. Our results demonstrate that HSYA significantly improves the survival area of perforator flaps, increases blood supply, reduces tissue edema, and increases mean vascular density. HSYA treatment promotes angiogenesis and inhibits oxidative stress, apoptosis, and autophagy in perforator flaps, suggesting many potential mechanisms for flap survival.

Keywords: Hydroxysafflor yellow A, multiterritory perforator flaps, autophagy, angiogenesis, oxidative stress, apoptosis

Introduction

Due to a lack of suitable local tissue, extensive skin defects caused by severe trauma, burns, large tumor resection, or ulcers present considerable surgical challenges [1, 2]. Perforator flap use has become one of the more important surgical methods for repair and reconstruction because it achieves a good aesthetic effect at the recipient site and minimizes injury to the donor area [3]. However, flap necrosis at the dynamic territory boundary is one of the most common postoperative complications in perforator flap transplantation [4-6]. Flap necrosis is related to an insufficient blood supply [7, 8], there is a possibility that cell death is also caused by ischemia-reperfusion injury (IRI) [9-11]. Previous reports stated that apoptosis and oxidative stress are the two main mechanisms of IRI in flap surgery, ultimately resulting in flap necrosis [12]. Given these proposed mechanisms, strategies to promote angiogenesis and reduce oxidative stress and apoptosis are expected to effectively ameliorate necrosis of multiterritory perforator flaps.

Autophagy is a homeostatic process that occurs in all eukaryotic cells [13]. In a dynamic circulatory system, autophagy produces new building blocks and energy for cell renewal and homeostasis [14]. However, inappropriate autophagy can impair angiogenesis [15]. We previously showed that inhibition of autophagy can promote angiogenesis and enhance perforator flap survival [16]. Moreover, growing evidence shows that products related to oxidative stress such as reactive oxygen species (ROS) can promote apoptosis and necrosis [17] and are important activators of autophagy [18, 19]. Reducing excessive autophagy during myocardial IRI can inhibit excessive apoptosis [20]. Therefore, inhibition of autophagy may be an effective strategy for improving perforator flap survival.

Hydroxysafflor yellow A (HSYA) is the main active substance extracted from safflower [21] and has been reported to exert a number of biological and pharmacological actions such as pro-angiogenesis, anti-inflammatory, and antioxidative effects [22, 23]. By promoting angiogene-

Hydroxysafflor yellow A enhances the vitality of multiterritory perforating flaps

sis, HSYA can improve cardiac dysfunction caused by ischemia in a mouse model of acute myocardial infarction [24]. HSYA alleviates secondary neuronal death by reducing oxidative stress and inflammation in rats with spinal cord compression injury [25]. HSYA was also shown to improve sepsis-induced apoptosis of CD4+T lymphocytes through anti-apoptotic effects [26]. Another group reported that HSYA protected cerebral microvascular endothelial cells from oxygen glucose deprivation/reoxygenation by inhibiting autophagy via the class I phosphoinositide 3-kinase/Akt/mammalian target of rapamycin signaling pathway [27]. Despite these benefits, the effects of HSYA on perforator flap survival are completely unknown. Based on the putative mechanism mentioned above, we hypothesized that HSYA may be an effective treatment for flap necrosis.

Materials and methods

Experimental reagents

HSYA (C₂₇H₃₂O₁₆; purity ≥98.05%) was procured from Med Chem Express (Shanghai, China). Primary antibodies against vascular endothelial growth factor (VEGF), CD34, heme oxygenase 1 (HO1), Microtubule-associated 1 protein light chain 3 (LC3), SQSTM1/p62, Bcl-2, and GAPDH were acquired from Abcam (ab52917, ab81289, ab68477, ab48394, ab56416, ab185002, and ab181602, respectively; Cambridge, UK). Rabbit monoclonal anti-SOD2, anti-Bax, anti-matrix metalloproteinase-9 (MMP9), anti-VPS34, and anti-CTSD antibodies were purchased from Proteintech Group (24127-1, 50599-2, 10375-2, 12452-1, and 21327-1, respectively; Chicago, IL, USA). Rabbit monoclonal anti-endothelial nitric oxide synthase (eNOS) and anti-cleaved caspase-3 antibodies were acquired from Cell Signaling Technology (32027 and 9611; Danvers, MA, USA). The rabbit monoclonal anti-cadherin5 (CDH5) antibody was purchased from Boster Biological Technology (A02632-2; Wuhan, China). Pentobarbital sodium, a hematoxylin and eosin staining kit, and DAB developer were obtained from Solarbio Science & Technology (Beijing, China). Horseradish peroxidase-conjugated immunoglobulin G (IgG) secondary antibody was acquired from Santa Cruz Biotechnology (Dallas, TX, USA). 4',6-Diamidino-2-phenylindole (DAPI) solution was obtained from Beyotime

Biotechnology (Jiangsu, China), and fluorescein isothiocyanate-conjugated IgG secondary antibody was acquired from Boyun Biotechnology (Nanjing, China). Superoxide dismutase (SOD), glutathione (GSH), and malondialdehyde (MDA) assay kits were obtained from Jiancheng Technology (Nanjing, China). Electrochemiluminescence Plus Reagent Kits and bicinchoninic acid (BCA) Protein Assay Kits were purchased from Thermo Fisher Scientific (Waltham, MA, USA).

Animals

A total of 48, healthy, 8-week-old Sprague Dawley rats (male, average weight 240-260 g), from the Experimental Animal Center of Wenzhou Medical University (License No. SCXK [ZJ] 2005-0019) were individually housed in standard experimental cages in an environment-controlled room (temperature 22-25°C, humidity 60-70%, 12-/12-hour light: dark cycle), and they were provided with contaminant-free feed and drinking water. All procedures involving rats were approved by the Animal Research Committee of Wenzhou Medical University (wydw2017-0022) and cared for in accordance with the Ethical Guidelines on Animal Experimentation of Laboratory Animals of China National Institutes of Health.

Flap animal model

Rats were intraperitoneally injected with 3% pentobarbital sodium (60 mg/kg) for anaesthetization [4]. Before surgery, their dorsal fur was removed with an electric shaver, followed by hair removal cream. The surgery was performed under sterile conditions. A deep circumflex iliac (DCI) artery flap approximately 2.5 × 11 cm² was created on the right side of each rat dorsum, as previously described [6]. In the DCI artery flap model, there are three vascular territories, including the lateral thoracodorsal (TD) vessel perforator, posterior intercostal (IC) vessel perforator, and DCI vessel perforator (**Figure 1**). Among these, the DCI vascular territory is anatomical, the IC vascular territory is a dynamic region, and the TD vascular territory is a potential region. The flap was elevated beneath the panniculus carnosus, and the second choke zone (SCZ) between the IC and TD was identified by transillumination. Only the DCI perforator was retained, and the TD and IC perforators were ligated. The flap was then sewn in situ

Hydroxysafflor yellow A enhances the vitality of multiterritory perforating flaps

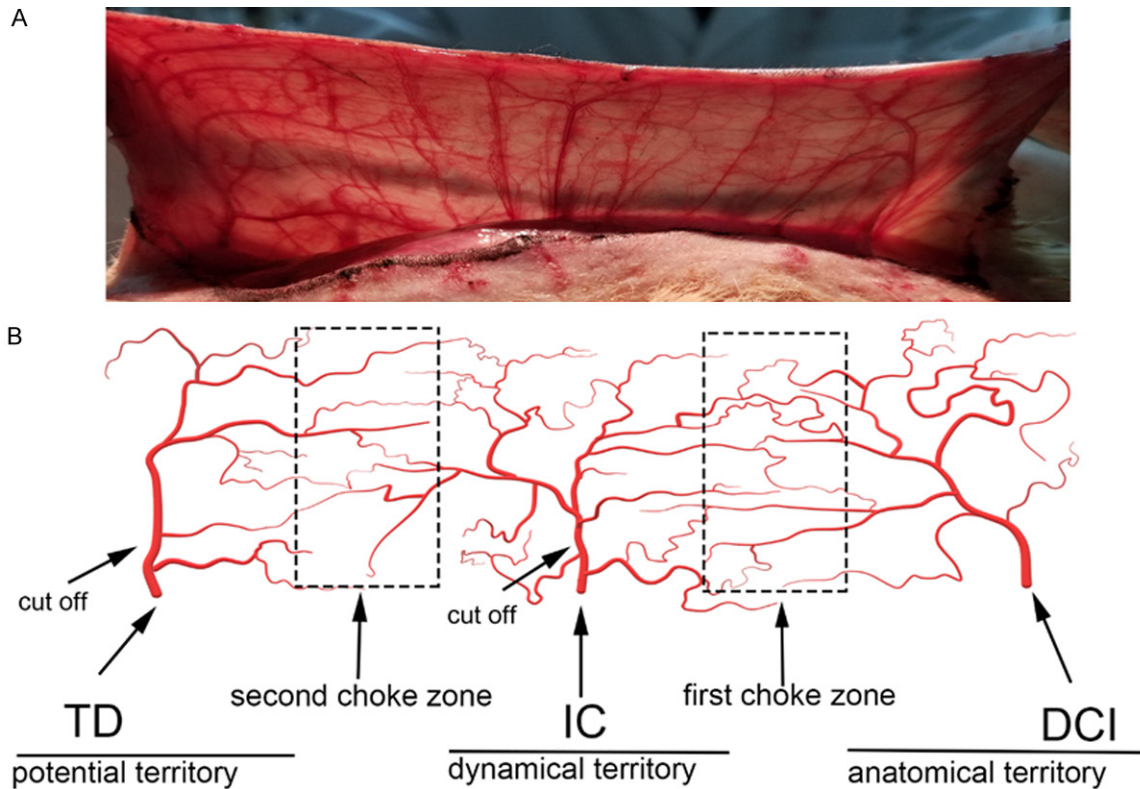


Figure 1. Diagrammatic representation of the vascular territory in the flap model. A. The perforating vessels of the three vascular territories can be observed after skin flap elevation. B. There were three vascular areas and two choke zones in the rat dorsal flap, including the deep circumflex iliac vessel (DCI), posterior intercostal vessel (IC) and lateral thoracodorsal vessel (TD), first choke zone (FCZ) and second choke zone (SCZ). From the DCI to the distal flap, the three territories are as follows: anatomical, dynamical, and potential. Choke vessels are potential and caliber-reduced vessels between the two vascular territories in the choke zone.

with 4-0 thread. Strict disinfection was performed before surgery, and aseptic procedures were observed during surgery.

Group assignment and drug administration

Forty-eight rats were randomly divided into control ($n = 24$) and HSYA ($n = 24$) groups. The HSYA group received HSYA dissolved in saline intraperitoneally at a dose of 20 mg/kg/day one a day after surgery until euthanasia [28]. The control group received equivalent normal saline daily. On postoperative day 7 (POD7), all rats were euthanized, and tissue samples were collected for analysis.

General evaluation of flap survival

Flap viability was assessed on POD7. A high-definition picture of the perforator flap was taken with a digital camera, and its appearance, color and texture were noted. Crusted, hardened, and dried regions were considered

necrotic areas. The survival area of the flap was measured with Image-Pro Plus v6.0 software (Media Cybernetics, Rockville, MD, USA). Flap viability was calculated with the following equation: (%) = (survival area of the flap/total area of the flap) \times 100%.

Assessment of tissue edema

Tissue edema is an important factor leading to flap necrosis and is thus an important index for its evaluation [29]. Tissue edema is reflected by flap water content. On POD7, the flap tissue was weighed, dehydrated at 50°C and weighed until the weight was stable for at least 2 days. The percentage of water content was measured as $([\text{wet weight} - \text{dry weight}]/\text{wet weight}) \times 100\%$.

Laser doppler blood flow (LDBF) measurement

Flap blood supply was evaluated by LDBF imaging on POD7 [30]. Six rats in each group were

Hydroxysafflor yellow A enhances the vitality of multiterritory perforating flaps

scanned with a laser Doppler machine (Moor Instruments, Axminster, UK) in a warm, quiet environment under anesthesia. LDBF signal markers (green, yellow, and red, from weak to strong) were used to show vascular flow and blood supply; skin with no blood supply was indicated in blue. Flap blood flow was quantified with Moor LDI Review software (ver. 6.1; Moor Instruments). The blood supply area was calculated as: LDBF signal area (green, yellow, and red). Each rat was assessed three times, and the mean value was used for analyses.

Hematoxylin and eosin (H&E) staining

The animals were sacrificed on POD7, and tissue samples were collected from the flap SCZ (1 × 1 cm) in 6 animals in each group. The samples were fixed in 4% paraformaldehyde for 24 hours and embedded in paraffin. The embedded tissue was fixed on a microtome and cut into 5- μ m-thick slices, which were subsequently stained with an H&E staining kit. We manually counted the number of microvessels per unit area (/mm²) under an optical microscope (\times 200 magnification, Olympus, Tokyo, Japan) to calculate the microvessel density (MVD). Six random fields were used from three random sections of each tissue sample for counting.

Immunohistochemistry (IHC)

Sections from the flap SCZ in each group (n = 6) were deparaffinized with xylene and rehydrated in a graded ethanol series. After washing, endogenous peroxidase activities were blocked with 3% H₂O₂, and antigen retrieval was carried out in 10.2 mM sodium citrate buffer for 20 min at 95°C. After blocking with 10% normal goat serum for 30 min, the sections were incubated with antibodies against CD34 (1:100), VEGF (1:200), CDH5 (1:100), cleaved caspase-3 (1:100), SOD (1:100), and p62 (1:100) overnight at 4°C. Finally, the sections were incubated with horseradish peroxidase-labeled goat anti-rabbit antibody and counterstained with hematoxylin. The sections were imaged at \times 200 magnification with a DP2-BSW image-acquisition system (Olympus). Integral absorbance quantitation with Image-Pro Plus v6.0 software as performed to compare CD34-positive blood vessels and protein expression levels. Six random fields were counted from three random sections of each tissue sample.

Immunofluorescence staining

Skin flap sections (n = 6) were deparaffinized and rehydrated in a graded ethanol series and incubated in 10% normal goat serum containing 0.3% Triton X-100 at room temperature for 30 min. After blocking, sections were incubated overnight with primary antibody LC3B (1:100) at 4°C, followed by incubation with tetramethylrhodamine-labeled goat anti-rabbit IgG antibody (1:100, Bioworld Technology, Nanjing, China) at room temperature for 1 hour. An anti-fluorescence quenching agent was added after DAPI staining for 2 min. Six random fields were used from three random sections of each tissue sample.

Western blot analysis

On POD7, skin samples (n = 6) from the SCZ were collected and stored at -80°C before western blotting. Six samples in each group were processed by extracting proteins with radioimmunoprecipitation lysis buffer. The extracts were quantified with BCA assays. Skin samples containing 60 μ g of protein were separated on 12% (w/v) gels and transferred onto polyvinylidene fluoride membranes. After blocking with 5% skimmed milk for 2 hours at room temperature, the membranes were incubated with the following appropriate primary antibodies at 4°C overnight: cadherin 5 (1:1,000), MMP9 (1:1,000), VEGF (1:1,000), eNOS (1:1,000), HO1 (1:1,000), SOD (1:1,000), cleaved caspase-3 (1:1,000), Bcl-2 (1:1,000), Bax (1:1,000), VPS34 (1:1,000), p62 (1:1,000), Beclin1 (1:1,000), CTSD (1:1,000), LC3B (1:500) and GAPDH (1:1,000). Membranes were then incubated at room temperature for 2 hours with a goat anti-rabbit secondary antibody. Immunoreactive signals were quantified using Image Lab 3.0 software (Bio-Rad, Hercules, CA, USA).

SOD activity, MDA content, and GSH level

SOD activity, MDA content and GSH levels were measured to assess oxidative stress status in the flap using testing kits (Jiancheng Technology, Nanjing, China). On POD7, specimens (n = 6) from the SCZ were obtained, weighed, homogenized, and diluted to 10% (v/v) in saline. SOD activity was evaluated following the xanthine oxidase method, MDA was measured via reaction with thiobarbituric acid at 95°C, and GSH

Hydroxysafflor yellow A enhances the vitality of multiterritory perforating flaps

level was quantified with the 5,5'-dithiobis method [31].

TUNEL staining

TdT-mediated dUTP nick-end labeling (TUNEL) was used to detect nuclear DNA breakage in the process of apoptosis. Staining was performed according to the instructions of the in situ cell death detection kit (F. Hoffmann-La Roche Ltd., Basel, Switzerland). Three random micro-fields of paraffin-embedded sections ($n = 6$) were observed at $200 \times$ magnification with a DP2-BSW image-acquisition system (Olympus).

Statistical analyses

All data are expressed as mean \pm standard deviation (SD). Statistical analysis was performed using SPSS software version 22.0 (IBM Corp., Armonk, NY, USA) with independent-sample t-tests. $P < 0.05$ indicates statistical significance.

Results

HSYA enhances perforator flap viability

Flap morphology was observed on POD7. The boundary between the viable and necrotic areas was obvious, and the color of the necrotic area was darker, accompanied by scabbing, hardening, and dryness (**Figure 2A**). Quantitative analysis showed that the average percentage of survival area in the HSYA group was significantly higher than that in the control group ($90.75 \pm 3.02\%$ and $76.92 \pm 4.02\%$, respectively; $P = 0.001$; **Figure 2B**). After measurement, the percentage of tissue water content in the HSYA group was significantly lower than that in the control group ($32.03\% \pm 1.70$ and $37.57\% \pm 3.27\%$, respectively; $P = 0.038$; **Figure 2C**). LDBF showed increased blood flow signal intensity in the HSYA group compared to the control group (**Figure 2D**). There was a significant difference in blood flow signal intensity between the HSYA and control groups (346.9 ± 39.51 PU and 254.4 ± 41.57 PU, respectively, $P = 0.004$, **Figure 2E**). H&E staining revealed that the HSYA group flaps had more microvessels than the control group (**Figure 2F**). The MVDs were calculated to quantify angiogenesis. The number of microvessels generated in the HSYA group ($27.40 \pm 3.39/\text{mm}^2$) was higher

than that in the control group ($19.02 \pm 3.83/\text{mm}^2$; $P = 0.007$; **Figure 2G**). Finally, vascular endothelial cells were labeled for CD34. The number of CD34-positive vessels in the HSYA group was significantly higher than that in the control group ($27.19 \pm 3.08/\text{mm}^2$ and $19.33 \pm 3.67/\text{mm}^2$, $P = 0.003$; **Figure 2G, 2I**).

HSYA promotes angiogenesis in perforator flaps

VEGF and CDH5 expression levels in perforator flaps were analyzed by IHC to quantify angiogenesis capacity. VEGF and CDH5 were expressed mainly in the blood vessels and stromal cells in the SCZ of all perforator flaps (**Figure 3A, 3C**). Quantification analysis showed that compared with control, HSYA treatment significantly promoted VEGF expression ($P = 0.002$; **Figure 3B**). Similarly, CDH5 expression was much higher in the HSYA group ($P = 0.005$; **Figure 3D**). Expression levels of CDH5, MMP9, and VEGF in the flap were analyzed by western blotting (**Figure 3E**). All three proteins were expressed at higher levels in the HSYA group compared to the control group ($P = 0.024$, 0.026 , and 0.018 , respectively; **Figure 3F-H**).

HSYA attenuated oxidative stress in perforator flaps

SOD expression was detected by IHC to assess oxidative stress in the SCZ of perforator flaps. As shown in **Figure 4A**, SOD levels in the vascular and stromal cells of the HSYA group were higher than those in the control group. This was found to be significant by measuring the integral absorbance of SOD ($P = 0.01$; **Figure 4B**). Levels of eNOS, HO1, and SOD in the flap were also analyzed by western blotting. (**Figure 4C**), and all three were higher in the HSYA group compared to the control group ($P = 0.008$, 0.034 , and 0.004 , respectively; **Figure 4D-F**). SOD activity in the HSYA group was higher than that in the control group (63.41 ± 3.56 , 43.94 ± 5.48 U/mg protein, respectively; $P = 0.005$; **Figure 4G**). The average MDA content in the HSYA group was 40.49 ± 5.52 nmol/mg protein, which was significantly lower than that in the control group (58.29 ± 7.44 , $P = 0.008$; **Figure 4H**). The level of GSH in the HSYA group (2.61 ± 0.22 nmol/mg protein) was significantly higher than that in the control group (1.61 ± 0.25 nmol/mg protein; $P = 0.036$; **Figure 4I**).

Hydroxysafflor yellow A enhances the vitality of multiterritory perforating flaps

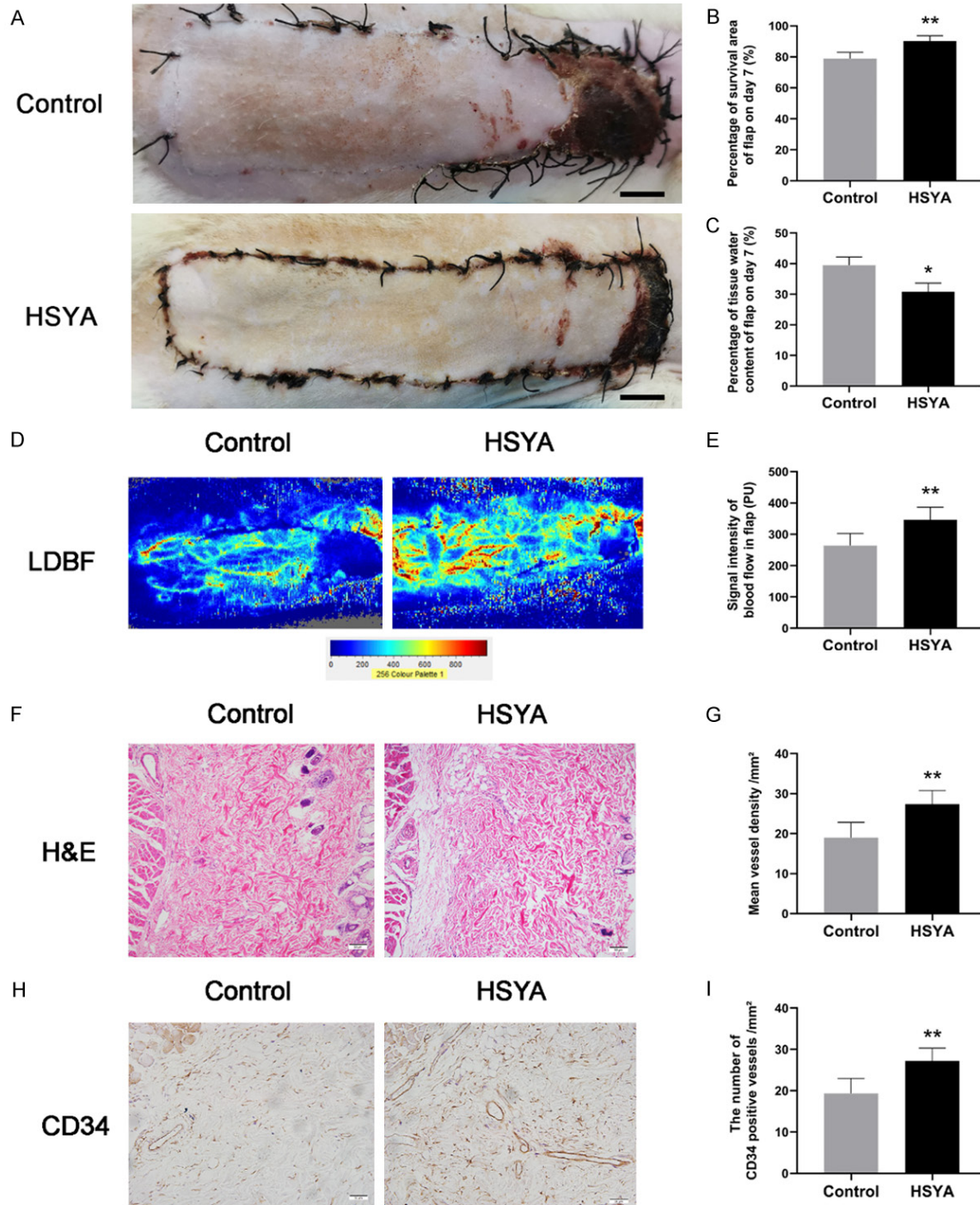


Figure 2. HSYA enhanced perforator flap viability, reduced tissue edema, and promoted flap angiogenesis. A. Digital photographs of flap survival in the control and HSYA groups were taken on POD7 (scale bar, 1.0 cm). B. The percentages of survival areas in the control and HSYA groups were quantified and analyzed. C. Histogram of percentage of tissue water content in each group. D. LDBF imaging of flaps in each group on POD7 to show the blood supply. Color palette shows different colors represent different signal intensity. The stronger the signal intensity, the greater the blood flow. E. Histogram of flap blood flow signal intensity. F. H&E staining showed the blood vessels in the SCZ of flaps in the control and HSYA groups (original magnification 200 ×; scale, 50 μm). G. The MVD in each group were quantified, analyzed, and plotted as a histogram (/mm²). H. IHC for CD34 showed the blood vessels of the SCZ of flaps in the control and HSYA groups (original magnification 200 ×; scale bar, 50 μm). I. Histogram of the percentage of CD34-positive vessels in each group. Data are expressed as mean ± SD, n = 6 per group. *P < 0.05 and **P < 0.01 vs. control.

Hydroxysafflor yellow A enhances the vitality of multiterritory perforating flaps

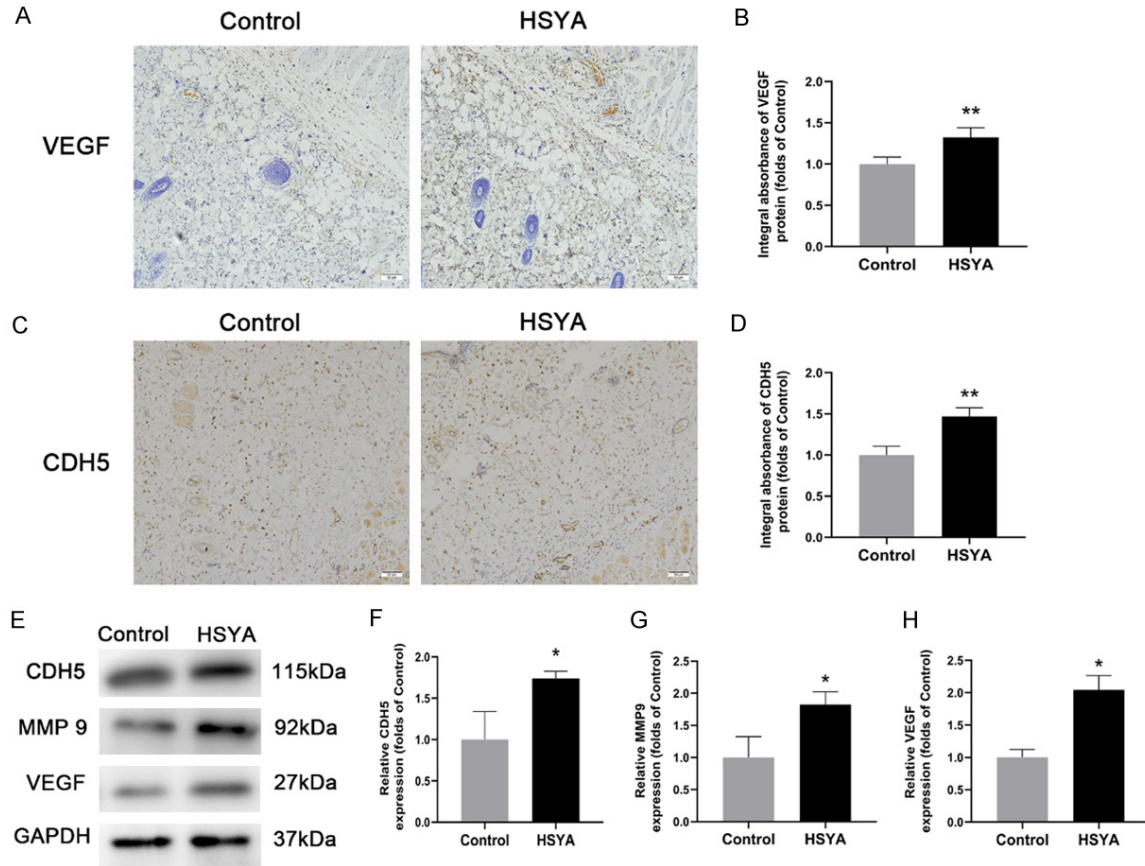


Figure 3. HSYA promotes angiogenesis in perforator flaps. On POD7, IHC was used to detect VEGF and CDH5 expression in the SCZs of flaps. Western blotting was used to detect the expression of CDH5, MMP9, and VEGF. A. IHC for VEGF expression in the SCZ of flaps (original magnification, 200 ×; scale, 50 μm). B. The optical density values of VEGF were quantified and analyzed. C. IHC for CDH5 expression in the SCZ of flaps (original magnification, 200 ×; scale, 50 μm). D. The optical density values of CDH5 were quantified and analyzed. E. The expressions of CDH5, MMP9, and VEGF protein in the SCZ of flaps of the control and HSYA groups were evaluated by western blotting. The gels were run under the same experimental conditions, and cropped blots are shown. The original image is in [Figure S1A](#). F-H. Optical density values of CDH5, MMP9, and VEGF were quantified and analyzed. Data are expressed as mean ± SD, n = 6 per group. *P < 0.05 and **P < 0.01 vs. control.

HSYA reduces apoptosis in perforator flaps

The number of TUNEL-positive cells in the control group was higher than that in the HSYA treatment group (**Figure 5A, 5B**). IHC was conducted to cleaved caspase-3 in the dermal layer of the SCZ of each group. The levels of cleaved caspase-3 in vessels and stromal cells were lower in the HSYA group compared to the control group (**Figure 5C**), and the integral absorbance was also lower (P < 0.001; **Figure 5D**). Western blotting was performed to detect Bcl-2, Bax, and cleaved caspase-3 expression in flaps (**Figure 5E**). The results showed that Bax and cleaved caspase-3 were decreased and the anti-apoptotic protein Bcl-2 was increased in the HSYA group compared with the

control group (P = 0.004, 0.012, and 0.009, respectively; **Figure 5F, 5H**).

HSYA inhibited autophagy in perforator flaps

Immunofluorescence staining for LC3II was performed to assess autophagosomes in cells in the SCZ of flaps. We labeled autophagosomes with LC3II antibody (red), and the nuclei were labeled with DAPI (blue) in the dermis of flaps (**Figure 6A**). Compared with control, the HSYA group exhibited lower numbers of LC3II-positive cells (**Figure 6B**). IHC for CTSD was conducted to detect the level of autophagic substrate in the SCZ of each group. As shown in **Figure 6C**, a lower level of CTSD was observed in the HSYA group compared to control. The

Hydroxysafflor yellow A enhances the vitality of multiterritory perforating flaps

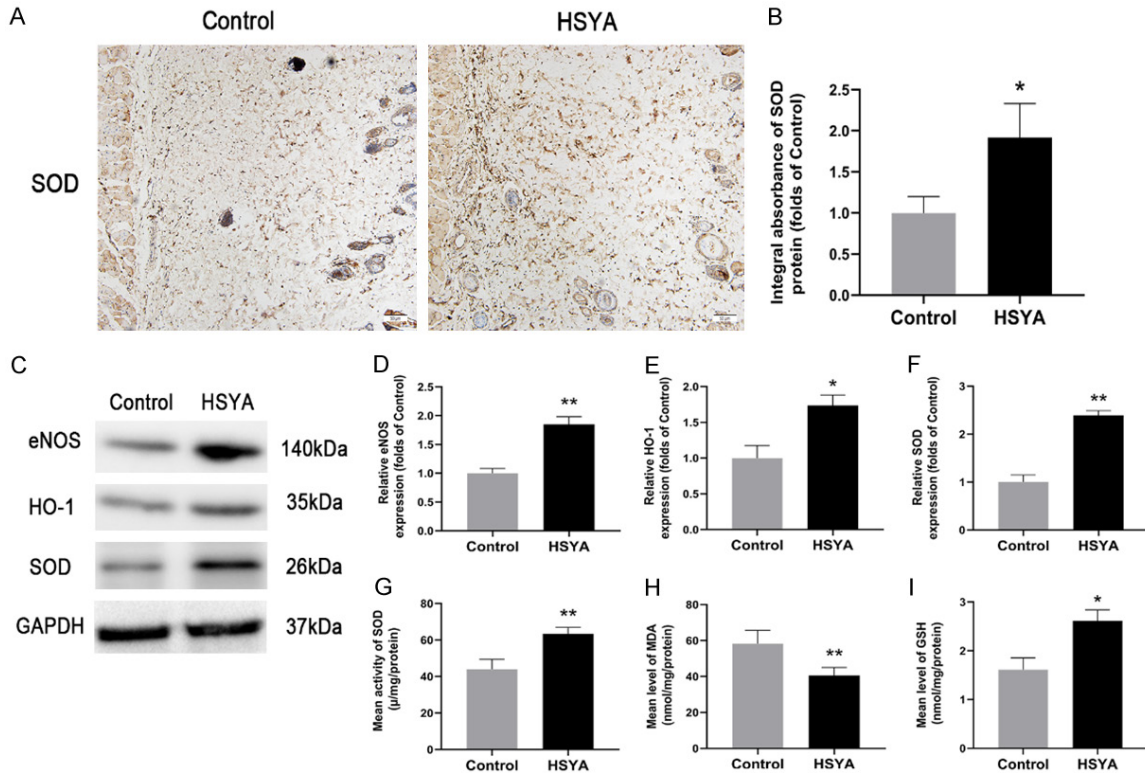


Figure 4. HSYA attenuated oxidative stress in perforator flaps. IHC for SOD was used to determine the level of oxidative stress in the SCZ of flaps. Western blotting was used to measure eNOS, HO1, and SOD. SOD, MDA, and GSH activities were measured on POD7. A. IHC for SOD expression in the SCZ of flaps (original magnification, 200 \times ; scale, 50 μm). B. The optical density values of SOD were quantified and analyzed. C. Protein levels of eNOS, HO1, and SOD in the SCZ of flaps were evaluated by western blotting. The gels were run under the same experimental conditions, and cropped blots are shown. The original image is in [Figure S1B](#). D-F. Optical density values of eNOS, HO1, and SOD were quantified and analyzed. G-I. Histograms of SOD activity, MDA content, and GSH level were analyzed with the xanthine oxidase method, 5,5'-dithiobis method, and modified TBA test, respectively. Data are expressed as mean \pm SD, n = 6 per group. *P < 0.05 and **P < 0.01 vs. control.

integral absorbance of CTSD in the HSYA group was significantly lower than that in the control group (P = 0.003; **Figure 6D**). Beclin1, Vps34, and LC3II/I are autophagy-related proteins; CTSD is a marker of autolysosomes; and p62 is an autophagic substrate protein. Western blotting was also performed to detect the expression levels of these proteins (**Figure 6E, 6F**). The results showed that the optical density values of Beclin1, LC3II, CTSD, and Vps34 were significantly lower in the HSYA group than in the control group (P = 0.004, 0.037, 0.014, and 0.008, respectively), whereas a higher level of p62 was detected in the HSYA group (P = 0.020; **Figure 6G**).

Discussion

HSYA is an active ingredient extracted from safflower [28]. Many recent studies have demon-

strated its efficacy in treating a variety of diseases [21, 24, 32, 33]. Large-area skin defects often need to be repaired with multi-territory perforator flaps [34, 35], but necrosis often limits the scope of flap resection [34, 35]. The causes of necrosis are inadequate blood supply and IRI [36-38]. In this study, HSYA significantly increased the survival of multi-territory perforator flaps by promoting angiogenesis and inhibiting oxidative stress, apoptosis, and excessive autophagy. These findings indicate that HSYA may have potential as a clinical agent to improve multi-territory perforator flap survival.

Both clinical practice and basic research showed that flap blood flow gradually decreases from the pedicle to the distal end, which may be the cause of necrosis [39, 40]. Some groups reported that increasing angiogenesis can

Hydroxysafflor yellow A enhances the vitality of multiterritory perforating flaps

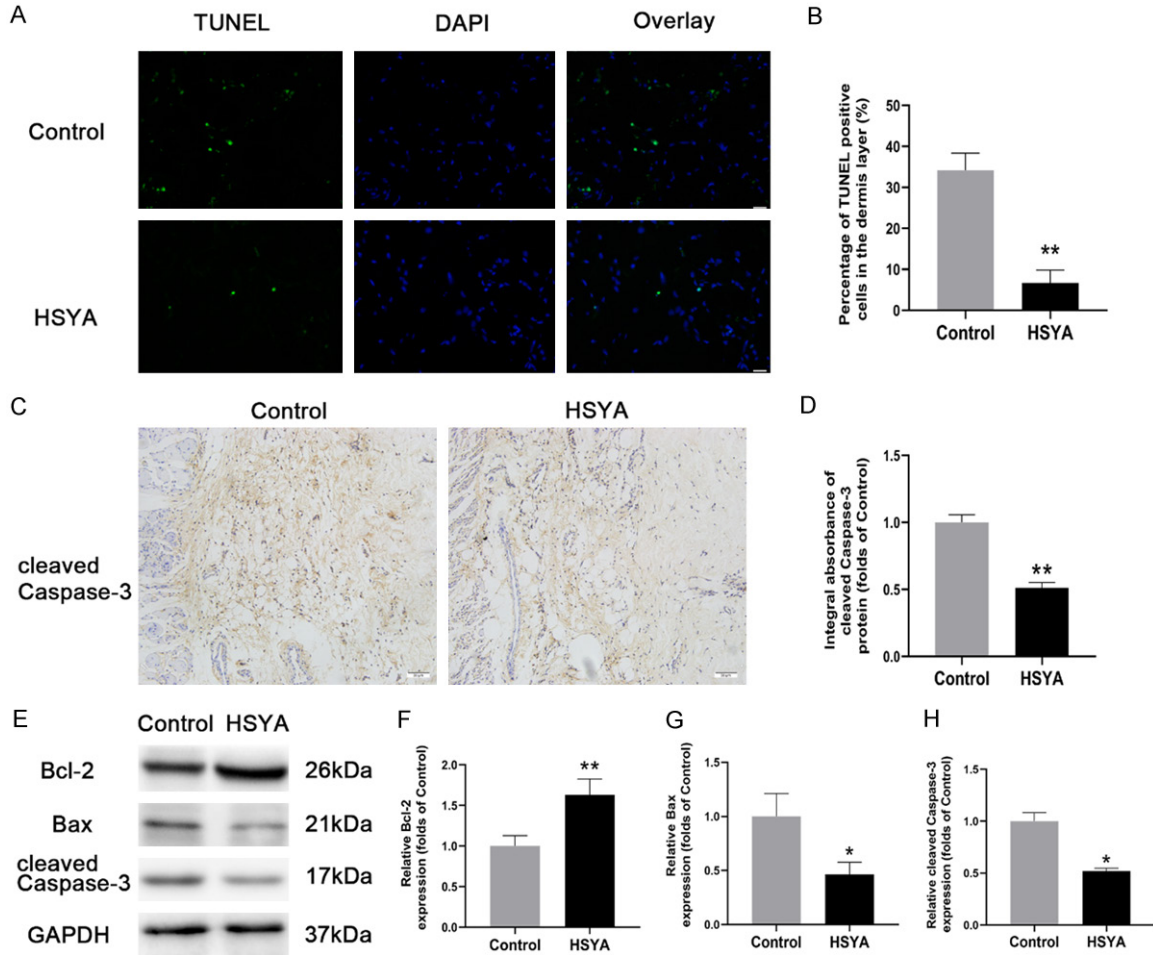


Figure 5. HSYA reduces apoptosis in perforator flaps. On POD7, apoptosis was evaluated with TUNEL kits. IHC for cleaved caspase-3 was used to assess apoptosis in the SCZ of flaps. Western blotting was used to measure Bcl-2, Bax, and cleaved caspase-3. A. TUNEL assays were performed to evaluate apoptosis in the SCZ of flaps. B. Apoptotic cell quantification. C. IHC for cleaved caspase-3 expression in the SCZ of flaps (original magnification, 200 ×; scale, 50 μm). D. The optical density values of cleaved caspase-3 were quantified and analyzed in each group. E. Protein levels of Bcl-2, Bax, and cleaved caspase-3 protein in the SCZ of flaps were evaluated by western blotting. The gels were run under the same experimental conditions, and cropped blots are shown. The original image is in Figure S1C. F-H. Optical density values of Bcl-2, Bax, and cleaved caspase-3 were quantified and analyzed. Data are expressed as mean ± SD, n = 6 per group. *P < 0.05 and **P < 0.01 vs. control.

improve perforator flap survival [41, 42]. HSYA can significantly promote human umbilical vein endothelial cell neovascularization and keratinocyte migration [43]. Similarly, our results showed that HSYA markedly increased microvessels in the SCZ of flaps, and blood perfusion on LDBF also improved. VEGF is the most important angiogenic factor known at present; it promotes neovascularization by stimulating endothelial cell proliferation and migration [44]. MMP9 stimulates the release of VEGF and promotes angiogenesis [45]. As a major adhesion protein in blood vessels, CDH5 is specifically expressed in the adhesion junctions of

endothelial cells [46]. We observed increases in the levels of CDH5, MMP9 and VEGF in the flaps of the HSYA group, and IHC confirmed that HSYA upregulated VEGF and CDH5 expression in the dermal layer of ischemic flaps. Collectively, our results indicate that HSYA enhances angiogenesis in perforator flaps.

During the postoperative reperfusion period, angiogenesis and blood flow bring oxygen but also produce ROS [47], which can cause vascular endothelial injury and vasoconstriction, as demonstrated in animal studies [48, 49]. High ROS levels can lead to protein denaturation,

Hydroxysafflor yellow A enhances the vitality of multiterritory perforating flaps

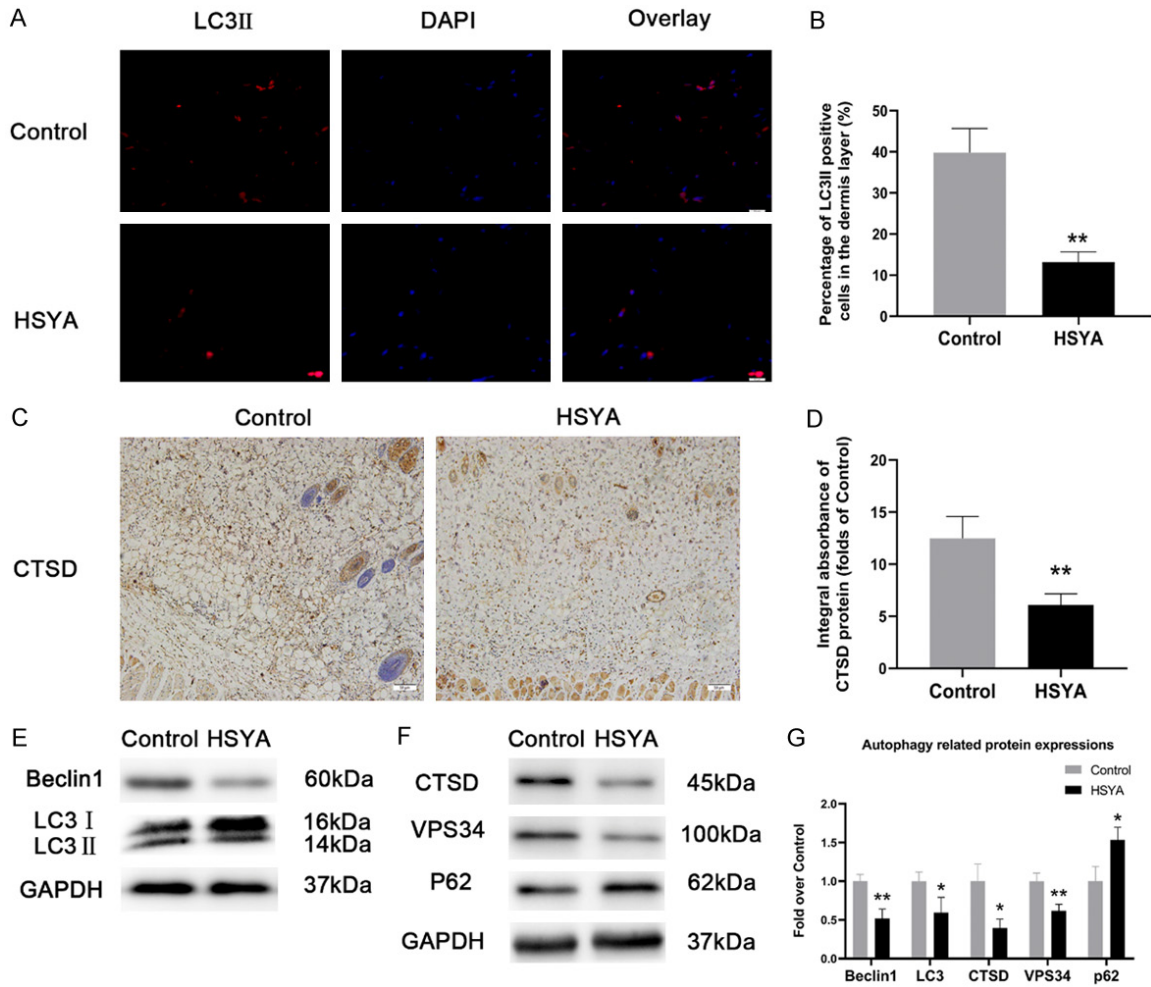


Figure 6. HSYA inhibited autophagy in perforator flaps. The level of autophagy in the SCZ of flaps was evaluated by IF for LC3II; IHC for CTSD; and western blotting for Beclin1, LC3II, CTSD, VPS34, and p62. A. Autophagosomes (red, LC3II) in cells in the SCZ of flaps; nuclei counterstained with DAPI (blue) (scale bar, 20 μ m). B. Histogram of the percentages of LC3II-positive cells. C. IHC for CTSD expression in the SCZ of flaps in each group (original magnification, 200 \times ; scale, 50 μ m). D. The optical density values of CTSD were quantified and analyzed. E, F. Protein levels of Beclin1, LC3II, CTSD, VPS34, and p62 in the SCZ of flaps were evaluated by western blotting. The gels were run under the same experimental conditions, and cropped blots are shown. The original image is in [Figure S1D](#). G. Optical density values of Beclin1, LC3II, CTSD, VPS34, and p62 were quantified and analyzed. Data are expressed as mean \pm SD, n = 6 per group. *P < 0.05 and **P < 0.01 vs. control.

lipid peroxidation of the cell membrane, and DNA damage [50, 51], as well as high levels of MDA [52]. SOD and GSH are antioxidants, and decreases in their activity can directly induce ROS accumulation and lead to oxidative damage [53]. eNOS regulates vascular function and antioxidant activity [54]. HO-1 is an antioxidant enzyme that can reduce oxygen free radicals [55]. HSYA was shown to increase SOD activity and GSH levels and decrease MDA levels in rats with traumatic brain injury [56]. In this study, HSYA exerted the same effects in skin flaps. In addition, treatment with HSYA in-

creased the expressions of eNOS, HO1, and SOD in the SCZ. The evidence indicates that HSYA can improve perforator flap survival by inhibiting oxidative stress.

Increasing evidence suggests that apoptosis can be induced during reperfusion [57, 58], and ROS cause DNA and mitochondrial damage, further promoting apoptosis [59]. Previous studies have shown that HSYA can reduce renal cell apoptosis and morphological changes in renal tissue [60]. In this study, we measured the expression of the anti-apoptotic factor Bcl-

Hydroxysafflor yellow A enhances the vitality of multiterritory perforating flaps

2, the pro-apoptotic factor Bax, and cleaved caspase-3 as indicators of the level of apoptosis [60, 61]. Our results showed increased Bcl2 level after HSYA treatment, and decreases in Bax and cleaved caspase-3. These results indicate that HSYA can reduce apoptosis in perforator flaps.

Autophagy can be activated by stimulating a variety of physiological and pathological factors to promote cell survival or death [62, 63]. Although autophagy can maintain tissue homeostasis [64], excessive autophagy damages cytoplasm components and organelles and hampers cell function [65]. We previously reported a significant difference in the level of autophagy-associated proteins before and after surgery in the SCZ and concluded that inhibition of autophagy promoted perforator flap survival [16]. Similarly, monotropein can accelerate wound healing by inhibiting oxidative stress-induced autophagy [66]. Interestingly, we found that HSYA also attenuated autophagy as indicated by the levels of the autophagy-related proteins Beclin1, LC3II, Vps34, autolysin-associated protein CTSD, and autophagy substrate protein p62. Immunofluorescence showed that LC3II and CTSD were lower in the HSYA group. In addition, Beclin1, LC3II, CTSD, and VPS34 expression were down-regulated, indicating an increase in the number of autophagosomes in flaps. The p62 level was higher than that in the control group, indicating reduced autophagy flux in the HSYA group. Collectively, these findings suggest that HSYA inhibited autophagy in perforator flaps.

Autophagy is a double-edged sword. On one hand, moderate autophagy triggered by mild to moderate hypoxia/ischemia has a protective effect and seems to prevent apoptosis [67]. On the other hand, high levels of autophagy caused by severe hypoxia or IRI may lead to self-digestion and eventually cell death [68]. Our previous study showed that autophagy inhibitors 3-methyladenine increases perforator flap survival [16]. Others reported that high glucose levels can upregulate autophagy and impair angiogenesis [15]. In addition, excessive autophagy can increase tissue injury, apoptosis, and ROS levels [69-71]. This is consistent with our findings that inhibition of autophagy is accompanied by decreased oxidative stress and apoptosis. Therefore, we suggest that

HSYA may inhibit oxidative stress and apoptosis by inhibiting autophagy in perforator flaps.

The molecular mechanisms by which HSYA promotes angiogenesis, reduces oxidative stress and apoptosis, and inhibits autophagy are still unclear. Further research is needed to understand these pathways and assess the clinical possibility of HSYA treatment following perforator flap transplantation.

HSYA promoted angiogenesis and suppressed oxidative stress and apoptosis. Autophagy was also inhibited in this process, which may be another potential mechanism for flap survival. In conclusion, HSYA contributed to a significant increase in perforator flap viability.

Acknowledgements

This research was sustained by China National Natural Science Foundation (80218123) and Zhejiang Province Natural Science Foundation of China (LY15H060010).

Disclosure of conflict of interest

None.

Address correspondence to: Weiyang Gao, Department of Orthopaedics, The Second Affiliated Hospital and Yuying Children's Hospital of Wenzhou Medical University, 109 West Xueyuan Road, Wenzhou 325000, Zhejiang, P. R. China. E-mail: weiyang-gaoi@126.com

References

- [1] Martí-Carvajal AJ, Gluud C, Nicola S, Simancas-Racines D, Reveiz L, Oliva P and Cedeo-Taborada J. Growth factors for treating diabetic foot ulcers. *Cochrane Database Syst Rev* 2015; CD008548.
- [2] Hashimoto I, Abe Y, Ishida S, Kashiwagi K, Mineda K, Yamashita Y, Yamato R, Toda A, Fukunaga Y, Yoshimoto S, Tsuda T, Nagasaka S and Keyama T. Development of skin flaps for reconstructive surgery: random pattern flap to perforator flap. *J Med Invest* 2016; 63: 159-62.
- [3] Yasir M, Wani AH and Zargar HR. Perforator flaps for reconstruction of lower limb defects. *World J Plast Surg* 2017; 6: 74-81.
- [4] Wang L, Jin Z, Wang J, Chen S, Dai L, Lin D, Wu L and Gao W. Detrimental effect of Hypoxia-inducible factor-1alpha-induced autophagy on

Hydroxysafflor yellow A enhances the vitality of multiterritory perforating flaps

- multiterritory perforator flap survival in rats. *Sci Rep* 2017; 7: 11791.
- [5] Harder Y, Amon M, Laschke MW, Schramm R, Rücker M, Wettstein R, Bastiaanse J, Frick A, Machens HG and Künthscher M. An old dream revitalised: preconditioning strategies to protect surgical flaps from critical ischaemia and ischaemia-reperfusion injury. *J Plast Reconstr Aesthet Surg* 2008; 61: 503-11.
- [6] Tao XY, Wang L, Gao WY, Ding J, Feng XL, Zhou ZW and Yang LH. The effect of inducible nitric oxide synthase on multiterritory perforator flap survival in rats. *J Reconstr Microsurg* 2016; 32: 643-649.
- [7] Kim JB, Eom JR, Lee JW, Lee J, Park HY and Yang JD. Utility of two surgical techniques using a lateral intercostal artery perforator flap after breast-conserving surgery: a single-center retrospective study. *Plast Reconstr Surg* 2019; 143: 477e-487e.
- [8] Myers MB and Cherry G. Causes of necrosis in pedicle flaps. *Plast Reconstr Surg* 1968; 42: 43-50.
- [9] Zhao G, Zhang X, Xu P, Mi JY and Rui YJ. The protective effect of Irisin against ischemia-reperfusion injury after perforator flap grafting in rats. *Injury* 2018; 49: 2147-2153.
- [10] Glass GE, Nanchahal J and Zamboni WA. Why haematomas cause flap failure: an evidence-based paradigm. *J Plast Reconstr Aesthet Surg* 2012; 65: 903-910.
- [11] Wang WZ, Baynosa RC and Zamboni WA. Update on ischemia-reperfusion injury for the plastic surgeon: 2011. *Plast Reconstr Surg* 2011; 128: 685e-92e.
- [12] van den Heuvel MG, Buurman WA, Bast A and van der Hulst RR. Review: ischaemia-reperfusion injury in flap surgery. *J Plast Reconstr Aesthet Surg* 2009; 62: 721-6.
- [13] Mizushima N, Komatsu M and Zamboni WA. Autophagy: renovation of cells and tissues. *Cell* 2011; 147: 728-741.
- [14] Choi AM, Ryter SW and Levine B. Autophagy in human health and disease. *N Engl J Med* 2013; 368: 651-62.
- [15] Kim KA, Shin YJ, Akram M, Kim ES, Choi KW, Suh H, Lee CH and Bae ON. High glucose condition induces autophagy in endothelial progenitor cells contributing to angiogenic impairment. *Biol Pharm Bull* 2014; 37: 1248-52.
- [16] Jin Z, Chen S, Wu H, Wang J, Wang L and Gao W. Inhibition of autophagy after perforator flap surgery increases flap survival and angiogenesis. *J Surg Res* 2018; 231: 83-93.
- [17] Chen L, Teng H, Zhang KY, Skalicka-Woźniak K, Georgiev MI and Xiao J. Agrimonolide and demethylagrimonolide induced HO-1 expression in HepG2 cells through Nrf2-transduction and p38 inactivation. *Front Pharmacol* 2016; 7: 513.
- [18] Morales CR, Pedrozo Z, Lavandero S and Hill JA. Oxidative stress and autophagy in cardiovascular homeostasis. *Antioxid Redox Signal* 2014; 20: 507-518.
- [19] Bhogal RH, Weston CJ, Curbishley SM, Adams DH and Afford SC. Autophagy: a cyto-protective mechanism which prevents primary human hepatocyte apoptosis during oxidative stress. *Autophagy* 2012; 8: 545-558.
- [20] Gao C, Wang R, Li B, Guo Y, Yin T, Xia Y, Zhang F, Lian K, Liu Y, Wang H, Zhang L, Gao E, Yan W and Tao L. TXNIP/redd1 signaling and excessive autophagy: a novel mechanism of myocardial ischemia/reperfusion injury in mice. *Cardiovasc Res* 2020; 116: 645-657.
- [21] Jiang S, Shi Z, Li C, Ma C and Wang C. Hydroxysafflor yellow A attenuates ischemia/reperfusion-induced liver injury by suppressing macrophage activation. *Int J Clin Exp Pathol* 2014; 7: 2595-608.
- [22] Ao H, Feng W and Peng C. Hydroxysafflor Yellow A: a promising therapeutic agent for a broad spectrum of diseases. *Evid Based Complement Alternat Med* 2018; 2018: 8259280.
- [23] Yu L, Duan Y, Zhao Z, He W, Xia M, Zhang Q and Cao X. Hydroxysafflor Yellow A (HSYA) improves learning and memory in cerebral ischemia reperfusion-injured rats via recovering synaptic plasticity in the hippocampus. *Front Cell Neurosci* 2018; 12: 371.
- [24] Zou J, Wang N, Liu M, Bai Y, Wang H, Liu K, Zhang H, Xiao X and Wang K. Nucleolin mediated pro-angiogenic role of hydroxysafflor yellow a in ischaemic cardiac dysfunction: post-transcriptional regulation of VEGF-A and MMP-9. *J Cell Mol Med* 2018; 22: 2692-2705.
- [25] Pei JP, Fan LH, Nan K, Li J, Dang XQ and Wang KZ. HSYA alleviates secondary neuronal death through attenuating oxidative stress, inflammatory response, and neural apoptosis in SD rat spinal cord compression injury. *J Neuroinflammation* 2017; 14: 97.
- [26] Wang J, Wang P, Gui S, Li Y, Chen R, Zeng R, Zhao P, Wu H, Huang Z and Wu J. Hydroxysafflor Yellow A attenuates the apoptosis of peripheral blood CD4 T lymphocytes in a murine model of sepsis. *Front Pharmacol* 2017; 8: 613.
- [27] Yang G, Wang N, Seto SW, Chang D and Liang H. Hydroxysafflor yellow a protects brain microvascular endothelial cells against oxygen glucose deprivation/reoxygenation injury: involvement of inhibiting autophagy via class I PI3K/Akt/mTOR signaling pathway. *Brain Res Bull* 2018; 140: 243-257.
- [28] Hu ZC, Xie ZJ, Tang Q, Li XB, Fu X, Feng ZH, Xuan JW, Ni WF and Wu AM. Hydroxysafflor yel-

Hydroxysafflor yellow A enhances the vitality of multiterritory perforating flaps

- low A (HSYA) targets the NF- κ B and MAPK pathways and ameliorates the development of osteoarthritis. *Food Funct* 2018; 9: 4443-4456.
- [29] Wu H, Ding J, Wang L, Lin J, Li S, Xiang G, Jiang L, Xu H, Gao W and Zhou K. Valproic acid enhances the viability of random pattern skin flaps: involvement of enhancing angiogenesis and inhibiting oxidative stress and apoptosis. *Drug Des Devel Ther* 2018; 12: 3951-3960.
- [30] Abraham A, Alabdali M, Alsulaiman A, Breiner A, Barnett C, Katzberg HD, Lovblom LE, Perkins BA and Brill V. Laser doppler flare imaging and quantitative thermal thresholds testing performance in small and mixed fiber neuropathies. *PLoS One* 2016; 11: e0165731.
- [31] Chen L, Zhou K, Chen H, Li S, Lin D and Zhou D. Calcitriol promotes survival of experimental random pattern flap via activation of autophagy. *Am J Transl Res* 2017; 9: 3642-3653.
- [32] Chen L, Xiang Y, Kong L, Zhang X, Sun B, Wei X and Liu H. Hydroxysafflor yellow A protects against cerebral ischemia-reperfusion injury by anti-apoptotic effect through PI3K/Akt/GSK3 β pathway in rat. *Neurochem Res* 2013; 38: 2268-2275.
- [33] Chen T, Chen N, Pang N, Xiao L, Li Y, Li R, Luo M, Deng X, Ren M, Wu J and Wang L. Hydroxysafflor Yellow A promotes angiogenesis via the Angiopoietin 1/ Tie-2 signaling pathway. *J Vasc Res* 2016; 53: 245-254.
- [34] Gao ZM, Lin DM, Wang Y, Li JJ, Chen S and Gao WY. Role of the NO/cGMP pathway in postoperative vasodilation in perforator flaps. *J Reconstr Microsurg* 2015; 31: 107-12.
- [35] Wang Y, Chen SY, Gao WY, Ding J, Shi W, Feng XL, Tao XY, Wang L and Ling DS. Experimental study of survival of pedicled perforator flap with flow-through and flow-end blood supply. *Br J Surg* 2015; 102: 375-381.
- [36] Ren H, Meng X, Yin J, Sun J, Huang Q and Yin Z. Ganoderma lucidum polysaccharide peptide attenuates skin flap ischemia-reperfusion injury in a thioredoxin-dependent manner. *Plast Reconstr Surg* 2018; 142: 23e-33e.
- [37] Kolbenschlag J, Sogorski A, Kapalschinski N, Harati K, Lehnhardt M, Daigeler A, Hirsch T and Goertz O. Remote ischemic conditioning improves blood flow and oxygen saturation in pedicled and free surgical flaps. *Plast Reconstr Surg* 2016; 138: 1089-1097.
- [38] Wu H, Chen H, Zheng Z, Li J, Ding J, Huang Z, Jia C, Shen Z, Bao G, Wu L, Mamun AA, Xu H, Gao W and Zhou K. Trehalose promotes the survival of random-pattern skin flaps by TFEB mediated autophagy enhancement. *Cell Death Dis* 2019; 10: 483.
- [39] Razzano S, Figus A, Marongiu F and Haywood R. Contralateral DIEV as an interpositional vein graft for venous supercharge in the salvage of a congested DIEP flap. *Microsurgery* 2016; 36: 263-264.
- [40] Miyamoto S, Minabe T and Harii K. Effect of recipient arterial blood inflow on free flap survival area. *Plast Reconstr Surg* 2008; 121: 505-513.
- [41] Kim SY, Rah DK, Chong Y, Lee SH and Park TH. Bilirubin provides perforator flap protection from ischaemia-reperfusion injury in a rat model: a preliminary result. *Int Wound J* 2016; 13: 870-7.
- [42] Bayati S, Russell RC and Roth AC. Stimulation of angiogenesis to improve the viability of pre-fabricated flaps. *Plast Reconstr Surg* 1998; 101: 1290-1295.
- [43] Gao SQ, Chang C, Niu XQ, Li LJ, Zhang Y and Gao JQ. Topical application of Hydroxysafflor Yellow A accelerates the wound healing in streptozotocin induced T1DM rats. *Eur J Pharmacol* 2018; 823: 72-78.
- [44] Ferrara N. VEGF and the quest for tumour angiogenesis factors. *Nat Rev Cancer* 2002; 2: 795-803.
- [45] Bellafiore M, Battaglia G, Bianco A, Farina F, Palma A and Paoli A. The involvement of MMP-2 and MMP-9 in heart exercise-related angiogenesis. *J Transl Med* 2013; 11: 283.
- [46] Rudini N, Felici A, Giampietro C, Lampugnani M, Corada M, Swirsding K, Garrè M, Liebnner S, Letarte M, ten Dijke P and Dejana E. VE-cadherin is a critical endothelial regulator of TGF-beta signalling. *EMBO J* 2008; 27: 993-1004.
- [47] Kerrigan CL and Stotland MA. Ischemia reperfusion injury: a review. *Microsurgery* 2010; 14: 165-175.
- [48] Manson PN, Anthenelli RM, Im MJ, Bulkley GB and Hoopes JE. The role of oxygen-free radicals in ischemic tissue injury in island skin flaps. *Ann Surg* 1983; 198: 87-90.
- [49] Im MJ, Hoopes JE, Yoshimura Y, Manson PN and Bulkley GB. Xanthine: acceptor oxidoreductase activities in ischemic rat skin flaps. *J Surg Res* 1989; 46: 230-234.
- [50] Shadel GS and Horvath TL. Mitochondrial ROS signaling in organismal homeostasis. *Cell* 2015; 163: 560-569.
- [51] Srinivas US, Tan BWQ, Vellayappan BA and Jeyasekharan AD. ROS and the DNA damage response in cancer. *Redox Biol* 2019; 25: 101084.
- [52] Zhang JM, Wang HC, Wang HX, Ruan LH, Zhang YM, Li JT, Tian S and Zhang YC. Oxidative stress and activities of caspase-8, -9, and -3 are involved in cryopreservation-induced apoptosis in granulosa cells. *Eur J Obstet Gynecol Reprod Biol* 2013; 166: 52-55.
- [53] Hagar H and Al Malki W. Betaine supplementation protects against renal injury induced by cadmium intoxication in rats: role of oxidative

Hydroxysafflor yellow A enhances the vitality of multiterritory perforating flaps

- stress and caspase-3. *Environ Toxicol Pharmacol* 2014; 37: 803-811.
- [54] Katusic ZS and Austin SA. Endothelial nitric oxide: protector of a healthy mind. *Eur Heart J* 2014; 35: 888-894.
- [55] Xu D, Chen L, Chen X, Wen Y, Yu C, Yao J, Wu H, Wang X, Xia Q and Kong X. The triterpenoid CDDO-imidazolide ameliorates mouse liver ischemia-reperfusion injury through activating the Nrf2/HO-1 pathway enhanced autophagy. *Cell Death Dis* 2017; 8: e2983.
- [56] Wang Y, Zhang C, Peng W, Xia Z, Gan P, Huang W, Shi Y and Fan R. Hydroxysafflor yellow A exerts antioxidant effects in a rat model of traumatic brain injury. *Mol Med Rep* 2016; 14: 3690-6.
- [57] Zhao ZQ, Nakamura M, Wang NP, Wilcox JN, Shearer S, Ronson RS, Guyton RA and Vinten-Johansen J. Reperfusion induces myocardial apoptotic cell death. *Cardiovasc Res* 2000; 45: 651-60.
- [58] Gottlieb RA, Burleson KO, Kloner RA, Babior BM and Engler RL. Reperfusion injury induces apoptosis in rabbit cardiomyocytes. *J Clin Invest* 1994; 94: 1621-8.
- [59] Burns AT, Davies DR, McLaren AJ, Cerundolo L, Morris PJ and Fuggle SV. Apoptosis in ischemia/reperfusion injury of human renal allografts. *Transplantation* 1998; 66: 872-876.
- [60] Bai J, Zhao J, Cui D, Wang F, Song Y, Cheng L, Gao K, Wang J, Li L, Li S, Jia Y and Wen A. Protective effect of hydroxysafflor yellow A against acute kidney injury via the TLR4/NF- κ B signaling pathway. *Sci Rep* 2018; 8: 9173.
- [61] Smith CM, Chen Y, Sullivan ML, Kochanek PM and Clark RS. Autophagy in acute brain injury: feast, famine, or folly? *Neurobiol Dis* 2011; 43: 52-59.
- [62] Bursch W. The autophagosomal-lysosomal compartment in programmed cell death. *Cell Death Differ* 2001; 8: 569-81.
- [63] Scherz-Shouval R, Shvets E, Fass E, Shorer H, Gil L and Elazar Z. Reactive oxygen species are essential for autophagy and specifically regulate the activity of Atg4. *EMBO J* 2007; 26: 1749.
- [64] Cuervo AM. Autophagy: many paths to the same end. *Mol Cell Biochem* 2004; 263: 55-72.
- [65] Huang Z, Han Z, Ye B, Dai Z, Shan P, Lu Z, Dai K, Wang C and Huang W. Berberine alleviates cardiac ischemia/reperfusion injury by inhibiting excessive autophagy in cardiomyocytes. *Eur J Pharmacol* 2015; 762: 1-10.
- [66] Wang C, Mao C, Lou Y, Xu J, Wang Q, Zhang Z, Tang Q, Zhang X, Xu H and Feng Y. Monotropein promotes angiogenesis and inhibits oxidative stress-induced autophagy in endothelial progenitor cells to accelerate wound healing. *J Cell Mol Med* 2018; 22: 1583-1600.
- [67] Decker RS and Wildenthal K. Lysosomal alterations in hypoxic and reoxygenated hearts. I. Ultrastructural and cytochemical changes. *Am J Pathol* 1980; 98: 425-44.
- [68] Gustafsson AB and Gottlieb RA. Eat your heart out: role of autophagy in myocardial ischemia/reperfusion. *Autophagy* 2008; 4: 416-421.
- [69] Matsui Y, Takagi H, Qu X, Abdellatif M, Sakoda H, Asano T, Levine B and Sadoshima J. Distinct roles of autophagy in the heart during ischemia and reperfusion: roles of AMP-activated protein kinase and Beclin 1 in mediating autophagy. *Circ Res* 2007; 100: 914-922.
- [70] Zheng B, Mao JH, Qian L, Zhu H, Gu DH, Pan XD, Yi F and Ji DM. Pre-clinical evaluation of AZD-2014, a novel mTORC1/2 dual inhibitor, against renal cell carcinoma. *Cancer Lett* 2015; 357: 468-475.
- [71] Vande Velde C, Cizeau J, Dubik D, Alimonti J, Brown T, Israels S, Hakem R and Greenberg AH. BNIP3 and genetic control of necrosis-like cell death through the mitochondrial permeability transition pore. *Mol Cell Biol* 2000; 20: 5454-5468.

Hydroxysafflor yellow A enhances the vitality of multiterritory perforating flaps

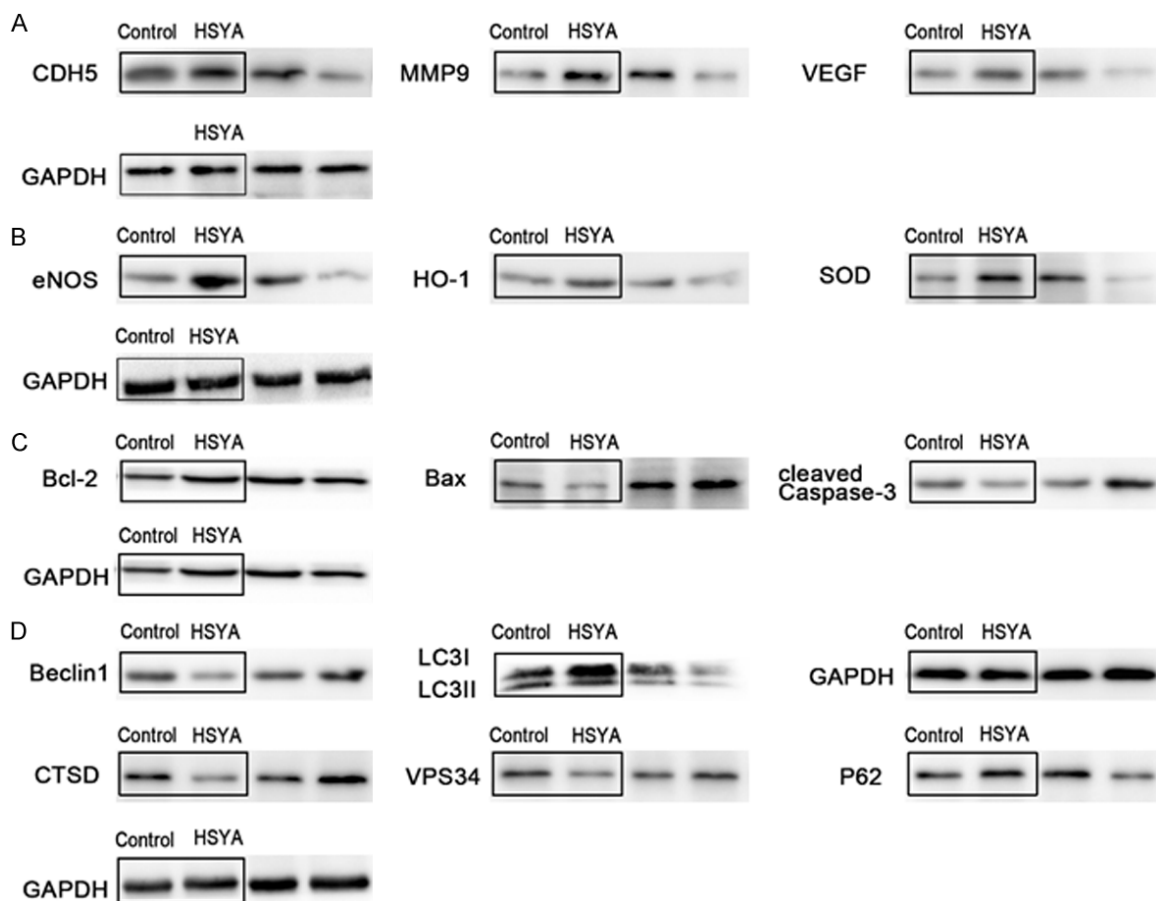


Figure S1. Original western blot images for each western blot in the study. A. The original gel images for **Figure 3E**. B. The original gel images for **Figure 4C**. C. The original gel images for **Figure 5E**. D. The original gel images for **Figure 5E, 5F**.